Quantifying ecological, morphological, and genetic variation to delimit species in the coast horned lizard species complex (*Phrynosoma*)

Adam D. Leaché[a,1], Michelle S. Koo[a], Carol L. Spencer[a], Theodore J. Papenfuss[a], Robert N. Fisher[b], and Jimmy A. McGuire[a]

[a]Museum of Vertebrate Zoology, 3101 Valley Life Sciences Building, University of California, Berkeley, CA 94720-3160; and [b]Western Ecological Research Center, U.S. Geological Survey, 4165 Spruance Road, Suite 200, San Diego, CA 92101

Communicated by David B. Wake, University of California, Berkeley, CA, June 8, 2009 (received for review April 20, 2009)

Lineage separation and divergence form a temporally extended process whereby populations may diverge genetically, morphologically, or ecologically, and these contingent properties of species provide the operational criteria necessary for species delimitation. We inferred the historical process of lineage formation in the coast horned lizard (*Phrynosoma coronatum*) species complex by evaluating a diversity of operational species criteria, including divergence in mtDNA (98 specimens; 2,781 bp) and nuclear loci (*RAG−1*, 1,054 bp; *BDNF* 529 bp), ecological niches (11 bioclimatic variables; 285 unique localities), and cranial horn shapes (493 specimens; 16 landmarks). A phylogenetic analysis of mtDNA recovers 5 phylogeographic groups arranged latitudinally along the Baja California Peninsula and in California. The 2 southern phylogeographic groups exhibit concordance between genetic, morphological, and ecological divergence; however, differentiation is weak or absent at more recent levels defined by phylogeographic breaks in California. Interpreting these operational species criteria together suggests that there are 3 ecologically divergent and morphologically diagnosable species within the *P. coronatum* complex. Our 3-species taxonomic hypothesis invokes a deep coalescence event when fitting the mtDNA genealogy into the species tree, which is not unexpected for populations that have diverged recently. Although the hypothesis that the 3 phylogeographic groups distributed across California each represent distinctive species is not supported by all of the operational species criteria evaluated in this study, the conservation status of the imperiled populations represented by these genealogical units remains critical.

evolution | geometric morphometrics | niche modeling | phylogeography | speciation

Lineage separation and divergence form a temporally extended process that may render populations reciprocally monophyletic for haplotype variation, reproductively isolated, ecologically divergent, or morphologically distinctive (1, 2). These contingent properties serve as the operational criteria that systematists use as evidence to delimit species, and they can arise at different times and in different orders during the process of lineage formation (3). This view of speciation is consistent with the general metapopulation lineage concept (2), which defines species as segments of population-level evolutionary lineages. Applying this lineage-based framework to delimit species shifts focus away from adopting a single operational criterion, which often yields conflicting views of species numbers, and increases the relevance for studying lineage separation by using multiple lines of evidence (3). Species delimitation is notoriously difficult when operational criteria support discordant species boundaries, but this is to be expected in recent or adaptive radiations (4). Evaluating multiple operational criteria not only increases our ability to detect recently separated lineages (5), but it can also provide stronger evidence for lineage separation when in agreement (3). In this study, we quantify multiple operational species criteria, including divergence in genetic, ecological, and morphological characters, as well as presence or absence of gene flow, to investigate lineage diversification in the coast horned lizard (*Phrynosoma coronatum*) species complex.

The *P. coronatum* species complex is distributed across a diversity of ecological zones spanning >2,200 km from the Cape Region of Baja California to Northern California (6). Most of the proposed species boundaries within the *P. coronatum* complex occur at junctions separating different ecological regions in Baja California (7), which implies that ecological diversification has played a critical role during lineage formation in this system. Ecological divergence represents an important stage during the process of lineage separation that has become increasingly feasible to quantify by using geographical information systems (GIS), and it is furthermore now possible to integrate these data within a phylogeographic framework (8–10). Predicting the geographic distributions of lineages can help to identify barriers to dispersal that are important because they can restrict gene flow and facilitate population divergence on an evolutionary timescale (11). Alternatively, an area of predicted overlap between parapatric populations may signify a contact zone where gene flow is ongoing (12).

The presence of prominent cranial horns is one of the most conspicuous anatomical features of *Phrynosoma* lizards (6), and these horns are presumed to function as a defense against predators (13). The *P. coronatum* complex exhibits a considerable degree of geographic variation in occipital and temporal horn shape (14), and prior species boundary hypotheses have relied solely on this and other morphological sources of variation to delimit species. More than 20 attempts to partition this geographic variation into a discrete taxonomy underlie a turbulent taxonomic history, with 1–6 species recognized at various times (15, 16). Despite this long history of taxonomic inquiry, cranial horn shape variation remains to be quantified and compared among populations by using rigorous statistical methods. The most recent morphological study recognized 4 species within the *P. coronatum* complex (17), each of which was presumed to be genetically isolated and to qualify as distinct evolutionary (18) or phylogenetic species (19). Linear measurements of cranial horns were included in this study; however, standard linear measurements are limited to detecting changes in relative length and do not capture the extent to which complex shapes, such as curved cranial horns, vary among populations. Geometric morphometric techniques provide a viable

Author contributions: A.D.L., M.S.K., C.L.S., T.J.P., and J.A.M. designed research; A.D.L., M.S.K., and C.L.S. performed research; A.D.L., T.J.P. and R.N.F. procured specimens; A.D.L., M.S.K., and C.L.S. analyzed data; and A.D.L., M.S.K., C.L.S., T.J.P., R.N.F., and J.A.M. wrote the paper.

The authors declare no conflict of interest.

Data deposition: Nucleotide sequences have been deposited in the GenBank database (accession nos. GQ279396–GQ929730).

[1]To whom correspondence should be sent at the present address: Genome Center and Section of Evolution and Ecology, One Shields Avenue, University of California, Davis, CA 95616. E-mail: aleache@ucdavis.edu.

This article contains supporting information online at www.pnas.org/cgi/content/full/0906380106/DCSupplemental.

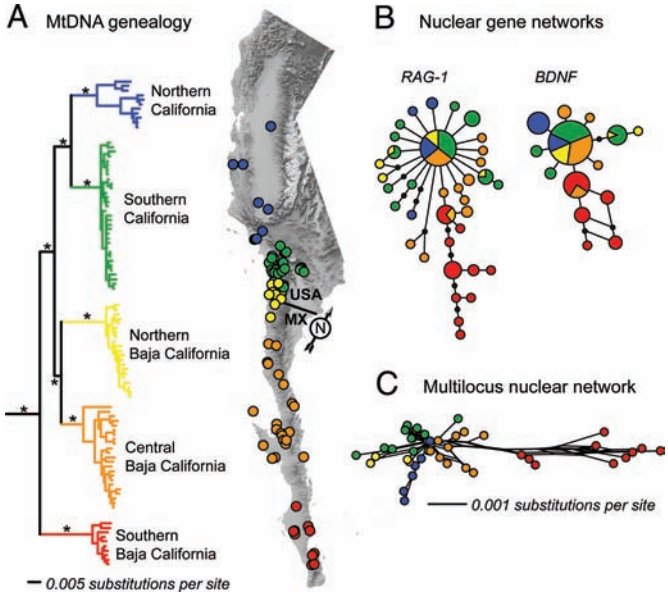

Fig. 1. Mitochondrial DNA genealogy (*A*), nuclear allele networks (*B*), and multilocus nuclear network showing the genetic distance among specimens (*C*) for the *P. coronatum* species complex. The mtDNA genealogy is based on a partitioned Bayesian analysis of 2,781 base pairs, and asterisks denote major clades with posterior probability values ≥0.99. Allele networks for the *RAG−1* and *BDNF* nuclear loci are based on statistical parsimony with a 95% connection significance. Specific locality data are provided in Table S5, and a detailed mtDNA genealogy and map illustrating the collecting locality of each sample is provided in Fig. S1.

alternative for analyzing complex shapes in multivariate space by retaining information about the relative spatial arrangements of the data throughout the analysis, which allows for the visualization of shape differences among groups (20). In this study, we conduct a geometric morphometric analysis of cranial horn shapes to determine whether the morphological evolution of these characters accompanies the formation of lineages in the *P. coronatum* species complex.

Results

Mitochondrial DNA Genealogy. A partitioned Bayesian phylogenetic analysis of mtDNA data provides strong support (posterior probabilities ≥0.99) for 5 major clades corresponding to 5 geographically parapatric groupings of populations arranged latitudinally along the Baja California Peninsula and in California [Fig. 1*A*; supporting information (SI) Fig. S1]. Because our primary focus is on the population-level entities being diagnosed by these haplotype clades, we refer to them as phylogeographic groups. The distributions of the 5 phylogeographic groups of the *P. coronatum* complex, from south to north, are as follows:

1. Southern Baja California: distributed across the Isthmus of La Paz from the Cape Region of Baja California and across the Magdalena Plain to the southern edge of the Vizcaino Desert.
2. Central Baja California: distributed across the Vizcaino Desert and the Central Gulf Coast and into the southern portion of the California Floristic Province to Colonia Guerrero.
3. Northern Baja California: distributed from Ensenada, Mexico, to San Diego County, California, where it overlaps marginally with the Southern California phylogeographic group.
4. Southern California: overlaps marginally with the Northern Baja California phylogeographic group in San Diego County and extends north to the Los Angeles Basin and San Gabriel Mountains and east to the edge of the Mojave Desert.
5. Northern California: distributed from the Los Angeles Basin to the northern portion of the California Central Valley and Coast Ranges.

The average sequence divergence (uncorrected) among the 5 major clades within the *P. coronatum* complex is 0.0464. The highest level of average divergence is between Southern Baja California and Northern California (0.0568), whereas the lowest level is between Central and Northern Baja California (0.03753). Levels of sequence divergence within the 5 phylogeographic groups range from a low of 0.00657 in Southern California to a high of 0.01689 in Northern California (average = 0.01027).

We conducted a Shimodaira–Hasegawa (SH) test (21) to determine whether the mtDNA data support the currently recognized species boundaries in the *P. coronatum* complex by using topological constraints that enforce the monophyly of the currently recognized species. The SH test results indicate that the topological constraints imposed to reflect the current taxonomy are significantly worse ($P < 0.0001$) than the unconstrained maximum likelihood topology ($ML_{best} = -9047.787297$; $ML_{constraints} = -9166.728912$; $D(LH) = -118.941615$).

Nuclear Gene Networks. Two nuclear loci (*RAG–1* and *BDNF*) show a substantial amount of allele sharing across the range of the *P. coronatum* complex, with each nuclear gene containing 1 allele that is widespread and shared among 4 of the 5 major phylogeographic groups (Fig. 1*B*). The nuclear alleles belonging to the Southern Baja California phylogeographic group cluster together, although several alleles from Central Baja California are shared with, or are only 1 mutational step removed from, this group (Fig. 1*B*). A multilocus nuclear gene network showing the genetic distance among specimens supports a clear separation between the Southern Baja California phylogeographic group and the remaining populations in the network (Fig. 1*C*). The resolution of the remaining portions of the multilocus network is too low to yield concordance between the multilocus network and the mtDNA genealogy (Fig. 1*C*).

Migration Estimation. Migration is not evident across the 2 phylogeographic boundaries in Baja California, but signatures of bidirectional migration are recovered for those in California (Fig. S2). Likelihood ratio tests comparing nested demographic models (22) reveal that a model assuming no migration is rejected only for the phylogeographic boundary between Southern California and Northern Baja California ($P = 0.040$; Table 1 and Table S1), which are also the only phylogeographic groups that show evidence of mtDNA haplotype overlap (Fig. 1*A*; Fig. S1).

Niche Divergence. Principal components analysis (PCA) of 11 bioclimatic variables (Table S2) reveals a high degree of niche overlap between the phylogeographic groups in California and in Northern Baja California (Fig. 2*A*). Niche separation between Southern Baja California and Central Baja California with respect to the remaining phylogeographic groups is evident, whereas the separation between Southern Baja California and Central Baja California is strong, but incomplete (Fig. 2*A*). The PCA analysis revealed 4 components collectively explaining >87% of the variation, with the first vector responsible for >40% of the variation (Fig. 2*A*; Table S3).

The climatic niche models predicted for the 5 phylogeographic groups exhibit varying degrees of overlap, with minimal overlap occurring at the extreme limits of the Southern Baja California and Central Baja California phylogeographic groups (Fig. S3). The 3 phylogeographic groups in California exhibit a substantial degree of overlap and overprediction beyond the known range of the species complex (Fig. S3). The relative influences of certain environmental parameters are often group specific. For example, the variable "mean temperature of coldest quarter" (bio11) makes a large contribution only to the model for Southern Baja California (88%), whereas the models for the groups that overlap spatially and show

Table 1. Phylogeographic comparisons of migration, morphological divergence, and niche differentiation in the *P. coronatum* complex

Phylogeographic comparison	Migration profile (LRT significance)	Morphometrics (male)	Morphometrics (female)	Bioclimate data	Niche identity (simulated mean, CI)
Northern California vs.	Nonzero peak	$F_{(1,91)} = 0.0507$	$F_{(1,92)} = 0.0386$	$F_{(1,303)} = 1.9029$	0.546
Southern California	$P \geq 0.322$	$P < 0.8223$	$P < 0.8447$	$P < 0.1688$	(0.753, 0.0508)
Southern California vs.	Nonzero peak	$F_{(1,47)} = 7.3432$	$F_{(1,73)} = 9.9786$	$F_{(1,159)} = 76.7841$	0.567
Northern Baja California	$P =$ **0.040**	$P <$ **0.0094**	$P <$ **0.0023**	$P <$ **0.0001**	(0.834, 0.0562)
Northern Baja California vs.	Peak at zero	$F_{(1,59)} = 46.6623$	$F_{(1,72)} = 34.1975$	$F_{(1,90)} = 305.1521$	0.38
Central Baja California	$P \geq 0.308$	$P <$ **0.0001**	$P <$ **0.0001**	$P <$ **0.0001**	(0.844, 0.0569)
Central Baja California vs.	Peak at zero	$F_{(1,84)} = 22.1170$	$F_{(1,82)} = 73.9413$	$F_{(1,82)} = 12.3785$	0.382
Southern Baja California	$P \geq 0.200$	$P <$ **0.001**	$P <$ **0.0001**	$P <$ **0.0007**	(0.832, 0.0561)

The posterior probability distributions for migration rates have nonzero peaks for the 2 northern phylogeographic breaks (indicating presence of gene flow), but a nested demographic model assuming no migration cannot be rejected for the Southern vs. Northern California comparison using a likelihood ratio test (LRT). MANOVA results for morphological and environmental differences are significant ($P < 0.05$; shown in bold) for all but the Southern California vs. Northern California comparisons. Niche identity tests comparing the observed similarity values (Warren's I) to simulated distributions (100 pseudoreplicates) reject the hypothesis that any parapatric phylogeographic groups are distributed in identical climate space.

evidence of nuclear gene flow in Southern California (i.e., Northern Baja California and Southern California) share reliance on the "precipitation of driest month" variable (bio14; Table S4).

Multivariate analysis of variance (MANOVA) tests on adjacent phylogeographic groups suggest that among-group environmental differences are significant ($P < 0.05$) for all comparisons, with the exception of the differences between Southern California and Northern California ($P < 0.168$; Table 1). Niche identity tests comparing observed similarity values [Warren's I; (23)] between adjacent phylogeographic groups suggest that niche similarity is higher in California and lower between groups in Baja California (Table 1). However, comparing the observed similarity values to simulated null distributions (100 pseudoreplicates) rejects the hypothesis that any adjacent phylogeographic groups are distributed in identical climate space (Table 1).

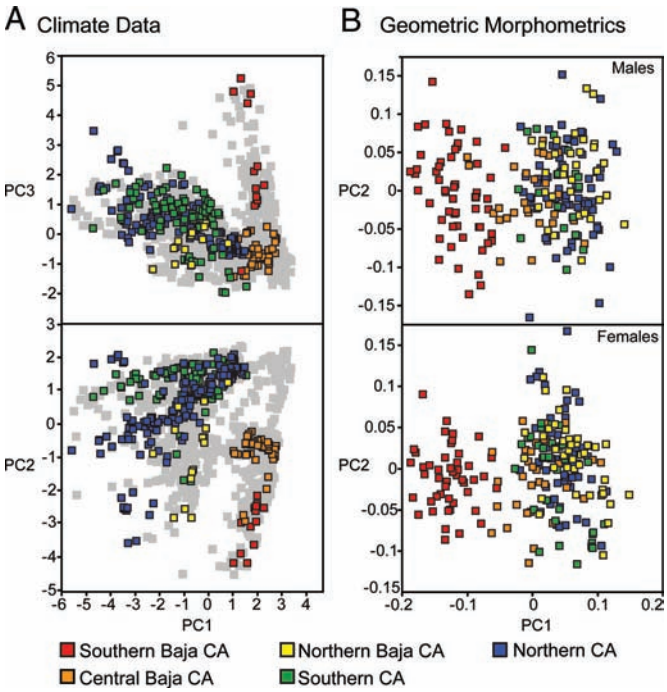

Fig. 2. Multivariate plots of the climate variables (*A*) and geometric morphometrics (*B*) for the *P. coronatum* complex. The climate data plots include 1,000 background points (shown in gray), drawn at random from the distribution of the *P. coronatum* complex (*A*). Variable loadings for the first, second, and third components for the climate data, respectively, are: mean temperature of coldest quarter, mean temperature of warmest quarter; temperature annual range, mean diurnal range; precipitation of driest month, precipitation of warmest quarter.

Geometric Morphometrics of Cranial Horn Morphology. The PCA plots generated by using geometric morphometric landmark data on cranial horns (Fig. 3*A*) show a strong, but incomplete, separation between Southern Baja California and Central Baja California, whereas the remaining phylogeographic groups overlap substantially (Fig. 2*B*). Variation in horn morphology is captured largely on the first vector (39%), whereas separation among groups on PC2 is limited, accounting for only 16% of the variation (Fig. 2*B*). Similar to the pattern observed with the environmental data, MANOVA tests comparing adjacent phylogeographic groups suggest that the differences in cranial horn shapes are significant ($P < 0.05$) for all comparisons, with the exception of the differences between Southern California and Northern California ($P < 0.8$; Table 1).

There are clear differences in cranial horn shape between the phylogeographic groups (Fig. 3). The curvature of the occipital horn, the largest and most conspicuous cranial horn in the armament of the *P. coronatum* complex, curves outward in the Southern Baja California phylogeographic group and is either parallel or curves inward toward the midline of the body in the more northern groups (Fig. 3*B*). Southern Baja California is distinctive in other horn characteristics as well, including a noticeably longer interoccipital horn and a shorter, laterally pointing posterior temporal horn (Fig. 3*B*). The 3 phylogeographic groups in California overlap substantially in cranial horn shape, whereas Central Baja California is often intermediate between these and Southern Baja California (Fig. 3*B*).

Discussion

Species Delimitation. Analyses of mtDNA, 2 nuclear loci, climatic niche models, and geometric morphometrics of cranial horn shapes in the *P. coronatum* species complex reveal that, at the deepest phylogenetic level, the geographical diagnoses of species boundaries are largely equivalent among the molecular genetic, ecological, and morphological criteria. The mtDNA genealogy (Fig. 1*A*) and multilocus nuclear network (Fig. 1*C*) support a congruent phylogeographic break in Southern Baja California, and there appears to be no nuclear gene flow across this boundary (Table 1). This phylogeographic break is accompanied by divergence in ecological niche (as measured by bioclimatic variables) and in cranial horn shapes (Fig. 2 *A* and *B*; Table 1). The morphometric study of Montanucci (17) supported the recognition of a distinctive Southern Baja California species, and the genetic, ecological, and geometric morphometric data presented here support that conclusion. These data add further evidence for recognizing multiple independent evolutionary lineages (i.e., separate species) within the

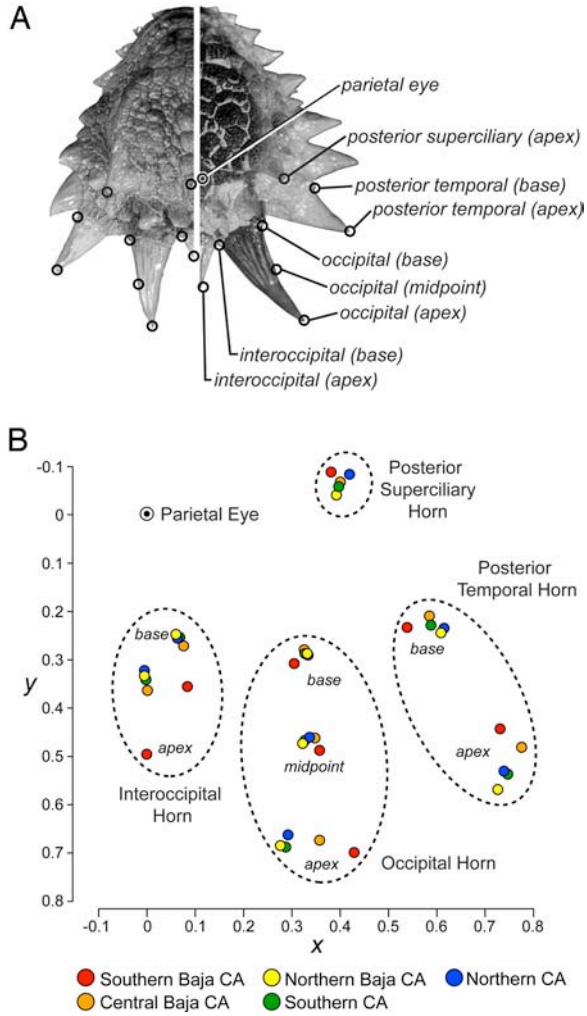

Fig. 3. Geographic variation in cranial horn shapes. (*A*) Cranial horn shape divergence and geometric morphometric landmark positions between *P. coronatum* complex specimens from Contra Costa County, California (*Left*; MVZ 33623) and Southern Baja California (*Right*; MVZ 100473). (*B*) The Southern Baja California phylogeographic group differs notably from all others in cranial horn shape. Mean landmark positions (average Bookstein coordinates; CS = 1) for each phylogeographic group are shown in relation to the parietal eye ($x = 0$, $y = 0$). Males and females produced similar results, and only results for females are shown here.

P. coronatum species complex. We recognize the Southern Baja California phylogeographic groups as a distinct species in the *P. coronatum* complex and follow Montanucci (17) in recognizing this lineage as *P. coronatum* (Blainville), with a type locality of Cape San Lucas, Baja California (24). The timing of this initial divergence event in the *P. coronatum* complex may be as recent as 2.3 myr (25). This species exhibits a number of properties suggesting that it is a separately evolving evolutionary lineage, including ecological divergence (26), allelic monophyly and exclusivity (19, 27, 28), reproductive isolation [e.g., lack of gene flow; (29)], and phenotypic differences (30).

Unlike the sharp character concordance observed across the phylogeographic break in Southern Baja California, patterns of character divergence are more obscured among the 4 remaining phylogeographic groups. The nuclear loci do not support the exclusivity of these phylogeographic groups (Fig. 1*C*), although this may indicate that the slowly evolving nuclear exons used in this study are inadequate for resolving relationships at this shallow temporal level. Despite the lack of genealogical resolution provided by the nuclear loci, these data provide pertinent information regarding migration, which is rejected for all but the Northern Baja and Southern California phylogeographic groups (Table 1). Although the signature of nuclear gene flow detected at this phylogeographic break could reflect current or historical processes, the spatial overlap of mtDNA haplotypes observed across this break argues for a lack of reproductive isolation among populations, and these independent lines of evidence suggest that the Northern Baja California and Southern California phylogeographic groups are not distinct evolutionary lineages. Evidence for recognizing the Northern California and Southern California phylogeographic groups as distinct evolutionary lineages is also weak, because these populations are not ecologically or morphologically distinct from one another (Table 1). However, the Central Baja California phylogeographic group satisfies all of the operational species criteria evaluated in this study and merits recognition as a distinct evolutionary lineage. This interpretation also follows from the species delimitation framework proposed by Bond and Stockman (31), which relies on the cohesion species criterion (32). Under this framework, parapatric populations are considered conspecific if they are ecologically interchangeable, which does not appear to be the case for Central Baja California with respect to Southern California to the north, nor with *P. coronatum* to the south (Table 1). According to the principles of priority, the name *Phrynosoma cerroense* (Stejneger) is applied to the Central Baja California phylogeographic group, with a type locality of Cedros Island, on the Pacific Coast of Baja California. *Phrynosoma blainvillii* (Gray) is applied to the remaining populations belonging to the Northern Baja California, Southern California, and Northern California phylogeographic groups, with a type locality of San Diego, San Diego County, California (14).

A cursory inspection of our 3-species hypothesis for the *P. coronatum* complex in relation to the mtDNA genealogy (Fig. 1*A*) reveals that haplotypes of P. *blainvillii* form a paraphyletic group, because the Northern Baja California haplotype clade of *P. blainvillii* is more closely related to *P. cerroense* than to the remaining clades contained within *P. blainvillii*. Although the mtDNA genealogy does provide strong support (≥0.99) for the inferred relationships, it is becoming increasingly appreciated that the genealogy inferred from any single locus can provide an inaccurate portrait of the species tree (33, 34). Reinterpreting the mtDNA genealogy within the context of the 3-species phylogeny illustrates that the case of *P. blainvillii* mtDNA paraphyly is rectified by invoking 1 instance of deep coalescence in the mtDNA locus (Fig. 4). Testing this "deep coalescence" hypothesis for the mtDNA genealogy requires the collection of additional multilocus nuclear data that are variable at this temporal level in conjunction with species tree inference methods that account for the process of lineage sorting (35, 36).

Conservation Implications. The *P. coronatum* species complex is undergoing population declines and local extirpations that are most pronounced in agricultural and urban areas. A primary factor contributing to these declines is the destruction of appropriate native chaparral habitats with sand substrates (37). The introduction of the invasive Argentine ant (*Linepithema humile*) also contributes to population declines by displacing the natural prey source, which consists of large harvester ants [e.g., *Pogonomyrmex*; (38)]. Experimental studies confirm that a diet consisting of only the introduced species causes starvation of captive lizards (39). Historically, populations in Southern California were heavily commercialized (40), and concerns regarding the impacts of continued international trade led to CITES Appendix II listing in 1975 (www.cites.org). In California, the 3 phylogeographic groups discovered within *P. blainvillii* represent important components of diversity that should be treated as distinct management units (distinct population segments) in future conservation and management decisions. In Baja California, *P. cerroense* and *P. coronatum*

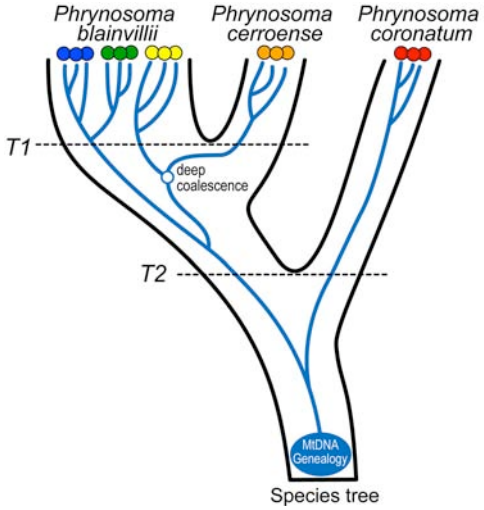

Fig. 4. Proposed species tree for the *P. coronatum* species complex and the contained mtDNA genealogy composed of 5 phylogeographic groups. The failure of all mtDNA haplotype lineages within *P. blainvillii* to coalesce between *T1* and the present results in an opportunity for deep coalescence between *P. blainvillii* and *P. cerroense*.

require special conservation considerations. Although many populations of *P. cerroense* are protected by extensive habitat reserves, heavy agriculture across the Magdalena Plain has the potential to eliminate *P. coronatum* from a significant portion of their range and cause a repeat of the massive population declines documented in California. This habitat loss is unfortunate, given that Baja California harbors a unique component of *Phrynosoma* diversity.

Materials and Methods

Genetic Data. We generated DNA sequence data for 98 specimens collected from throughout their range in California ($n = 63$) and Baja California ($n = 35$) (Table S5). We sequenced the entire mitochondrial *ND1* (969 bp) and *ND2* (1,033 bp) protein-coding genes and an 800-bp fragment of the 12S rRNA gene. We also sequenced 2 protein-coding nuclear genes, including 1,100 bp of recombination activating gene-1 (*RAG−1*) and 700 bp of brain-derived neurotrophic factor (*BDNF*). We collected complete data for most specimens (Table S5). New primer sequences developed for this study include an internal *ND2* primer (phrynoND2int: 5′-CAACAGCCCTCCTAACAATAGCCATA-3′), an internal *ND1* primer (phrynoND1int: 5′-CTAACAGACCTAAACCTAGGC-3′), and a modified version of the external *ND1* primer tMet (phrynotMet: 5′-GGCTCATTAGTAGAGGAGGGGTTTAAACCAAC-3′). The remaining primer sequences, lab protocols, and DNA alignment methods for the 12S rRNA data are provided in Leaché and McGuire (41). We included 7 species to represent outgroup taxa, including *Phrynosoma asio*, *Phrynosoma cornutum*, *Phrynosoma hernandesi*, *Phrynosoma mcallii*, *Phrynosoma modestum*, *Phrynosoma orbiculare*, and *Phrynosoma solare*.

Phylogenetic Analysis. We conducted phylogenetic analyses in a Bayesian framework by using mrBayes v3.1.2 (42). We separated the data into 7 partitions corresponding to the 12S rRNA gene (partition 1), first, second, and third codon positions for *ND1* (partitions 2, 3, and 4, respectively), and first, second, and third codon positions for *ND2* (partitions 5, 6, and 7, respectively). We used the Akaike information criterion (AIC) in MrModeltest v2.2 (43) to determine the best-fit nucleotide substitution model for each data partition (Table S6). Analyses were run with 4 chains (using default heating values) for 40 million generations, sampling every 1,000 generations. We implemented convergence diagnostics using the program AWTY (44).

We tested the morphometric-based taxonomy proposed by Montanucci (17) using the SH test (21). The maximum-likelihood tree constraining the monophyly of the 4 species recognized by Montanucci (17) was compared with an ML tree containing no topological constraints. We implemented the SH test using PAUP v.4.0b10 with 10,000 RELL bootstrap replicates and the GTR+I+Γ model of nucleotide substitution. We also implemented a partitioned SH test in RAxML v 7.0.4 (45) using the same data partitioning strategy used in our Bayesian phylogenetic analysis, with the exception that the GTR+Γ model was applied to each partition.

Allele and Multilocus Networks. We constructed allele networks for the nuclear loci (*BDNF* and *RAG−1*) using statistical parsimony with a 95% connection significance in the program TCS v1.21 (46). To infer haplotypes, we determined the phase of nuclear genotypes computationally using the program PHASE v2.1 (47, 48). We constructed a multilocus genetic network representing the relationships among specimens by converting the distance matrices for alleles from the separate nuclear loci into an organism matrix using the program POFAD v1.03 (49). The reconstructed organism network was visualized by using the NeighborNet algorithm (50) in SplitsTree v4.6 (51). We present the reconstructed organism network based on uncorrected patristic distances, but we also explored networks that incorporated corrected distance matrices using models selected by using the AIC.

Migration Estimation. We used the *RAG−1* and *BDNF* nuclear loci to determine whether any phylogeographic groups are exchanging migrants by testing nested models of population divergence in the program IMa (22). Assumptions of the IM model are that the loci under study are neutral and have not undergone intragenic recombination. We tested for intragenic recombination using the difference of sums of squares (DSS) test in TOPALi v2.5 (52), and deviations from neutrality were tested with the HKA test (53) by using the program DnaSP v4.10.4 (54). HKA tests for neutrality were not significant, and there is no evidence for recombination in either nuclear locus according to the DSS test. We ran 10 replicate IMa analyses (each using different starting seeds and 12 concurrent chains) for 10 million steps after an initial burn-in phase of 100,000 generations. Nested models of population divergence were compared by using likelihood ratio tests (22).

Environmental Data. Occurrence data were supplied by the samples from the genetic analyses augmented with museum records acquired from the database portal HerpNET (www.herpnet.org; accessed on November 29, 2007). Localities with a maximum georeferencing uncertainty of >10 km were excluded, leaving 285 unique sample localities used in the analysis. Minimum convex polygons circumscribing the geographic distribution of each mtDNA clade were used to assign HerpNET samples to phylogeographic groups and to define the area of analysis for climatic data sampling. All GIS tasks used ArcGIS 9.2 (ESRI) with bioclimatic variables from the Worldclim v1.4 dataset (55). Eight of the 19 bioclimatic variables were highly correlated [Pearson correlation coefficient (r) > 0.75; methods follow Rissler et al. (56)], and we used 11 bioclimatic variables for all analyses (Table S2).

Niche Modeling. We used Maxent v3.1 (57, 58) to generate predictive distribution models based on known occurrence samples and their corresponding environmental variables. Maxent is an appropriate choice for our data compared with other distributional modeling methods, because it provides robust performance with small sample sizes of presence-only data (59). We used the genetic samples as our presence-only dataset (the training set) with the bioclimatic variables to create distribution models by using default parameters in Maxent. The modeling calculations used the environmental data from the minimum convex polygon study area and then projected onto a broader geographic area encompassing western North America. We conducted multivariate statistical analyses of the environmental variables using R v2.6.0 and JMP v7 (SAS). We performed PCA to test whether the phylogeographic groups are discernible based on the bioclimatic variables without a priori designation of groups, and we tested for significant differences between groups using MANOVA.

Niche Identity Tests. We used niche identity tests (23) to test the null hypothesis that parapatric phylogeographic groups are distributed in identical environmental space. Given that environmental niche models make no biological assumptions of microhabitat use or species interactions, Warren et al. (23) proposed a mathematical approach that scales similarity from 0 (no overlap) to 1 (complete overlap), which we call Warren's I. We generated 100 simulated distribution models based on random replacement between samples of phylogeographic groups to test the null hypothesis that parapatric groups are distributed in identical environmental space.

Geometric Morphometrics of Cranial Horn Morphology. We examined cranial horn morphology in 493 specimens (245 females; 248 males; Table S7). Digital images of each specimen were obtained by using a flat-bed scanner, and the x, y coordinates of 16 landmarks (Fig. 3*A*) from the cranial horns and head plus 2 ruler landmarks were recorded from each image by using TPSDIG (60). We used the IMP software package (www3.canisius.edu/sheets/morphsoft.html) for image visualization and statistical analysis. We calculated the average value for symmetric landmarks (e.g., landmark positions on opposite sides of the head) using the program BigFix, resulting in 9 landmarks for each specimen (2 baseline and 7 averaged landmarks). We then generated Procrustes superimpositions for each

specimen using CoordGen (20). We used PCA to determine whether any morphological groupings were detectable without the a priori designation of groups, and we tested for significant differences in cranial horn shapes between parapatric phylogeographic groups using a 1-way MANOVA in JMP 7.0 (SAS).

ACKNOWLEDGMENTS. For tissue loans, we thank B. Hollingsworth and D. Wood (San Diego Society of Natural History, San Diego), R. Murphy and R. MacCulloch (Royal Ontario Museum, Toronto, ON, Canada), J. Vindum (California Academy of Sciences, San Francisco), G. Busteed and P. Johnson (U.S. National Park Service), W. Hodges, T. Reeder, E. Ervin, and R. Young. We are indebted to the collection managers at the California Academy of Sciences, Los Angeles County Museum, Museum of Vertebrate Zoology (MVZ) (Berkeley, CA), and the Smithsonian Institute (Washington, DC) for participating in the HerpNET data portal and for providing access to specimens. We thank H. Constable (HerpNET) for providing georeferenced data, N. Winters for scanning lizards at the MVZ, and D. L. Warren for modifying ENMtools to accommodate our data. We thank the Conservation Program of ESRI for donating GIS software. The use of trade, product, or firm names in this publication is for descriptive purposes only and does not imply endorsement by the U.S. Government. This work was funded in part by National Science Foundation Grant DEB 0330750 (to J.A.M.) and grants from The Nature Conservancy, California Department of Fish and Game, California Department of Parks and Recreation, Metropolitan Water District, U.S. Fish and Wildlife Service, and U.S. Department of Defense (to R.N.F.).

1. Harrison (1998) *Endless Forms: Species and Speciation*, eds Howard DJ, Berlocher SH (Oxford Univ Press, Oxford), pp 19–31.
2. de Queiroz K (1998) *Endless Forms: Species and Speciation*, eds Howard DJ, Berlocher SH (Oxford Univ Press, Oxford), pp 57–75.
3. de Queiroz K (2007) Species concepts and species delimitation. *Syst Biol* 56:879–886.
4. Wake DB (2006) Problems with species: Patterns and processes of species formation in salamanders. *Ann Mo Bot Gard* 93:8–23.
5. Sites JW, Marshall JC (2003) Delimiting species: A Renaissance issue in systematic biology. *Trends Ecol Evol* 18:462–470.
6. Sherbrooke WC (2003) *Introduction to Horned Lizards of North America* (Univ of California Press, Berkeley).
7. Grismer LL (2002) *Amphibians and Reptiles of Baja California Including Its Pacific Islands and the Islands in the Sea of Cortez* (Univ of California Press, Berkeley).
8. Kidd DM, Ritchie MG (2006) Phylogeographic information systems: Putting the geography into phylogeography. *J Biogeogr* 33:1851–1865.
9. Richards CL, Carstens BC, Knowles LL (2007) Distribution modeling and statistical phylogeography: An integrative framework for generating and testing alternative biogeographical hypotheses. *J Biogeogr* 34:1833–1845.
10. Rissler LJ, Apodaca JJ (2007) Adding more ecology into species delimitation: Ecological niche models and phylogeography help define cryptic species in the black salamander (*Aneides flavipunctatus*). *Syst Biol* 56:924–942.
11. Wiens JJ (2004) Speciation and ecology revisited: Phylogenetic niche conservatism and the origin of species. *Evolution (Lawrence, Kans)* 58:193–197.
12. Cicero C (2004) Barriers to sympatry between avian sibling species (Paridae: *Baeolophus*) in local secondary contact. *Evolution (Lawrence, Kans)* 58:1573–1587.
13. Young KV, Brodie ED, Jr, Brodei ED, III (2004) How the horned lizard got its horns. *Science* 304:65.
14. Klauber LM (1936) The horned toads of the coronatum group. *Copeia* 1936:103–110.
15. Jennings MR (1988) *Phrynosoma coronatum*. *Cat Am Amphib Reptiles* 428:1–5.
16. Brattstrom BH (1997) Status of the subspecies of the coast horned lizard, *Phrynosoma coronatum*. *J Herpetol* 31:434–436.
17. Montanucci RR (2004) Geographic variation in *Phrynosoma coronatum* (lacertilia, Phrynosomatidae): Further evidence for a peninsular archipelago. *Herpetologica* 60:117–139.
18. Wiley EO (1978) The evolutionary species concept reconsidered. *Syst Zool* 27:17–26.
19. Cracraft J (1983) Species concepts and speciation analysis. *Curr Ornithol* 1:159–187.
20. Zelditch ML, Swiderski DL, Sheets HD, Fink WL (2004) *Geometric Morphometrics for Biologists: A Primer* (Elsevier Academic, London).
21. Shimodaira H, Hasegawa M (1999) Multiple comparisons of log-likelihoods with applications to phylogenetic inference. *Mol Biol Evol* 16:1114–1116.
22. Hey J, Nielsen R (2007) Integration within the Felsenstein equation for improved Markov chain Monte Carlo methods in population genetics. *Proc Natl Acad Sci USA* 104:2785–2790.
23. Warren DL, Glor RE, Turelli M (2008) Environmental niche equivalency versus conservatism: Quantitative approaches to niche evolution. *Evolution (Lawrence, Kans)* 62:2868–2883.
24. Smith HM, Taylor EH (1950) Type-localities of Mexican reptiles and amphibians. *Univ Kansas Sci Bull* 33:313–380.
25. Leaché AD, Crews SC, Hickerson MJ (2007) Two waves of diversification in mammals and reptiles of Baja California revealed by hierarchical Bayesian analysis. *Biol Lett* 3:646–650.
26. Van Valen L (1976) Ecological species, multispecies, and oaks. *Taxon* 25:233–239.
27. Mishler BD (1985) The morphological, developmental, and phylogenetic basis of species concepts in bryophytes. *Bryologist* 88:207–214.
28. Baum DA, Shaw KL (1995) *Experimental and Molecular Approaches to Plant Biosystematics*, eds Hoch PH, Stevenson AG (Missouri Botanical Garden, St. Louis), pp 289–303.
29. Mayr E (1942) *Systematics and the Origin of Species* (Columbia Univ Press, New York).
30. Sokal RR, Crovello TJ (1970) The biological species concept: A critical evaluation. *Am Nat* 104:127–153.
31. Bond JE, Stockman AK (2008) An integrative method for delimiting cohesion species: Finding the population-species interface in a group of Californian trapdoor spiders with extreme genetic divergence and geographic structuring. *Syst Biol* 57:628–646.
32. Templeton AR (1998) *Endless Forms: Species and Speciation*, eds Howard DJ, Berlocher SH (Oxford Univ Press, Oxford), pp 32–41.
33. Pamilo P, Nei M (1988) Relationships between gene trees and species trees. *Mol Biol Evol* 5:568–583.
34. Degnan JH, Rosenberg NA (2006) Discordance of species trees with their most likely gene trees. *PLoS Genet* 2:762–768.
35. Maddison WP (1997) Gene trees in species trees. *Syst Biol* 46:523–536.
36. Edwards SV, Liu L, Pearl DK (2007) High-resolution species trees without concatenation. *Proc Natl Acad Sci USA* 104:5936–5941.
37. Fisher RN, Suarez AV, Case TJ (2002) Spatial patterns in the abundance of the coastal horned lizard. *Conserv Biol* 16:205–215.
38. Suarez AV, Bolger DT, Case TJ (1998) The effects of fragmentation and invasion on the native ant community in coastal Southern California. *Ecology* 16:2041–2056.
39. Suarez AV, Case TJ (2002) Bottom-up effects on persistence of a specialist predator: Ant invasions and horned lizards. *Ecol Appl* 12:291–298.
40. Jennings MR (1987) Impact of the curio trade for San Diego horned lizards (*Phrynosoma coronatum blainvillii*) in the Los Angeles Basin, California: 1885–1930. *J Herpetol* 21:356–358.
41. Leaché AD, McGuire JA (2006) Phylogenetic relationships of horned lizards (*Phrynosoma*) based on nuclear and mitochondrial data: Evidence for a misleading mitochondrial gene tree. *Mol Phylogenet Evol* 39:628–644.
42. Ronquist F, Huelsenbeck JP (2003) MrBayes 3: Bayesian phylogenetic inference under mixed models. *Bioinformatics* 19:1572–1574.
43. Nylander JAA (2004) *MrModeltest v2* (Evolutionary Biology Centre, Uppsala Univ, Uppsala).
44. Nylander JAA, Wilgenbusch JC, Warren DL, Swofford DL (2008) AWTY (are we there yet?): A system for graphical exploration of MCMC convergence in Bayesian phylogenetics. *Bioinformatics* 24:581–583.
45. Stamatakis A (2006) RAxML-VI-HPC: Maximum likelihood-based phylogenetic analysis with thousands of taxa and mixed models. *Bioinformatics* 22:2688–2690.
46. Clement M, Posada D, Crandall KA (2000) TCS: A computer program to estimate gene genealogies. *Mol Ecol* 9:1657–1659.
47. Stephens M, Smith N, Donnelly P (2001) A new statistical method for haplotype reconstruction from population data. *Am J Hum Genet* 68:978–989.
48. Stephens M, Scheet P (2005) Accounting for decay of linkage disequilibrium in haplotype inference and missing-data imputation. *Am J Hum Genet* 76:449–462.
49. Joly S, Bruneau A (2006) Incorporating allelic variation for reconstructing the evolutionary history of organisms from multiple genes: An example from *Rosa* in North America. *Syst Biol* 55:623–636.
50. Bryant D, Moulton V (2004) Neighbor-Net: An agglomerative method for the construction of phylogenetic networks. *Mol Biol Evol* 21:255–265.
51. Huson DH, Bryant D (2006) Application of phylogenetic networks in evolutionary studies. *Mol Biol Evol* 23:254–267.
52. McGuire G, Wright F (2000) TOPAL 2.0: Improved detection of mosaic sequences within multiple alignments. *Bioinformatics* 16:130–134.
53. Hudson RR, Kreitman M, Aguade M (1987) A test of neutral molecular evolution based on nucleotide data. *Genetics* 116:153–159.
54. Rozas J, Sánchez-DelBarrio JC, Messeguer X, Rozas R (2003) DnaSP, DNA polymorphism analyses by the coalescent and other methods. *Bioinformatics* 19:2496–2497.
55. Hijmans RJ, Cameron SE, Parra JL, Jones PG, Jarvis A (2005) Very high resolution interpolated climate surfaces for global land areas. *Int J Climatol* 25:1965–1978.
56. Rissler LJ, Hijmans RJ, Graham CH, Moritz C, Wake DB (2006) Phylogeographic lineages and species comparisons in conservation analyses: A case study of California herpetofauna. *Am Nat* 167:655–666.
57. Phillips SJ, Dudik M, Schapire RE (2004) A maximum entropy approach to species distribution modeling. *Proc Twenty-First Int Conf Machine Learn* 69:83–99.
58. Phillips SJ, Anderson RP, Schapire RE (2006) Maximum entropy modeling of species geographic distributions. *Ecol Model* 190:231–259.
59. Elith J, et al. (2006) Novel methods improve prediction of species' distributions from occurrence data. *Ecography* 29:129–151.
60. Rohlf FJ (2001) Comparative methods for the analysis of continuous variables: Geometric interpretations. *Evolution (Lawrence, Kans)* 50:2143–2160.

Supporting Information

Leaché et al. 10.1073/pnas.0906380106

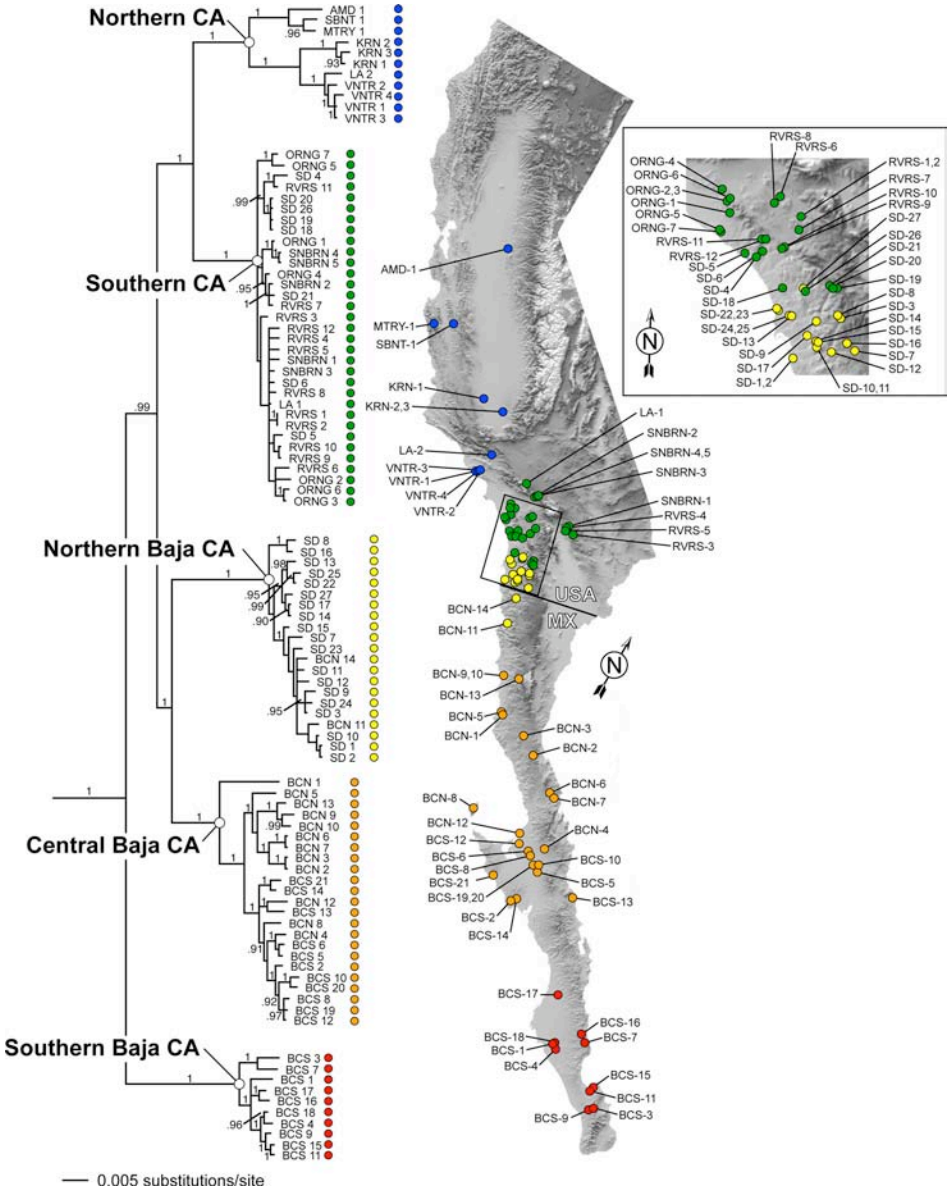

Fig. S1. Mitochondrial DNA genealogy for the *Phrynosoma coronatum* complex based on a partitioned Bayesian analysis of 2,781 base pairs. Posterior probability values ≥0.50 are indicated on nodes. Specific locality data are provided in Table S5.

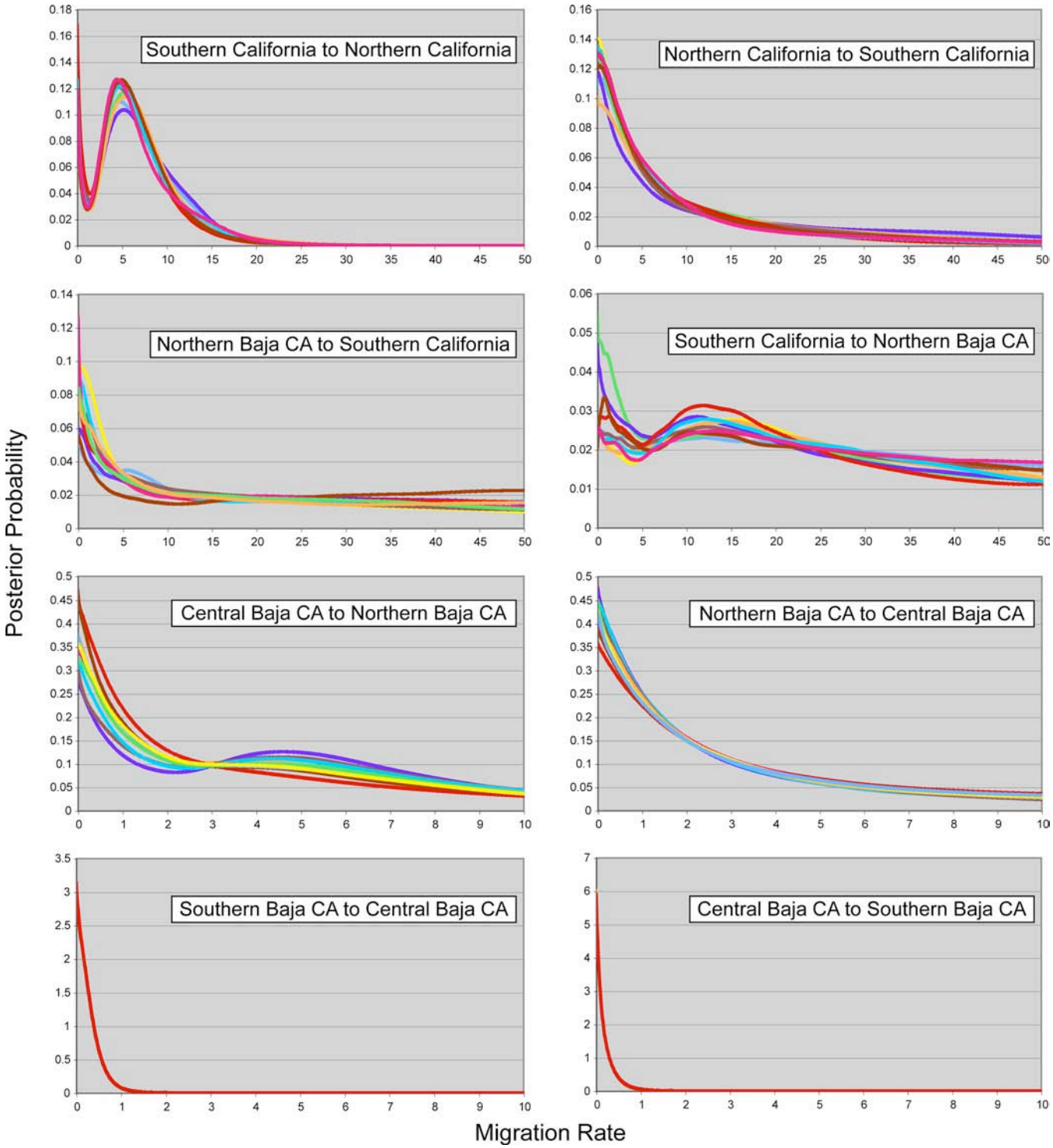

Fig. S2. Marginal posterior probability distributions of the bidirectional migration rates (scaled by the neutral mutation rate) between phylogeographic groups in the *P. coronatum* complex. The results from 10 independent IMa runs using different starting seeds are superimposed. Migration is not evident across the 2 phylogeographic boundaries in Baja California (strong peaks at zero), but signatures of bidirectional migration are recovered for those in California (nonzero peaks). A model assuming no migration is only rejected for the phylogeographic boundary between Southern California and Northern Baja California (Table S1).

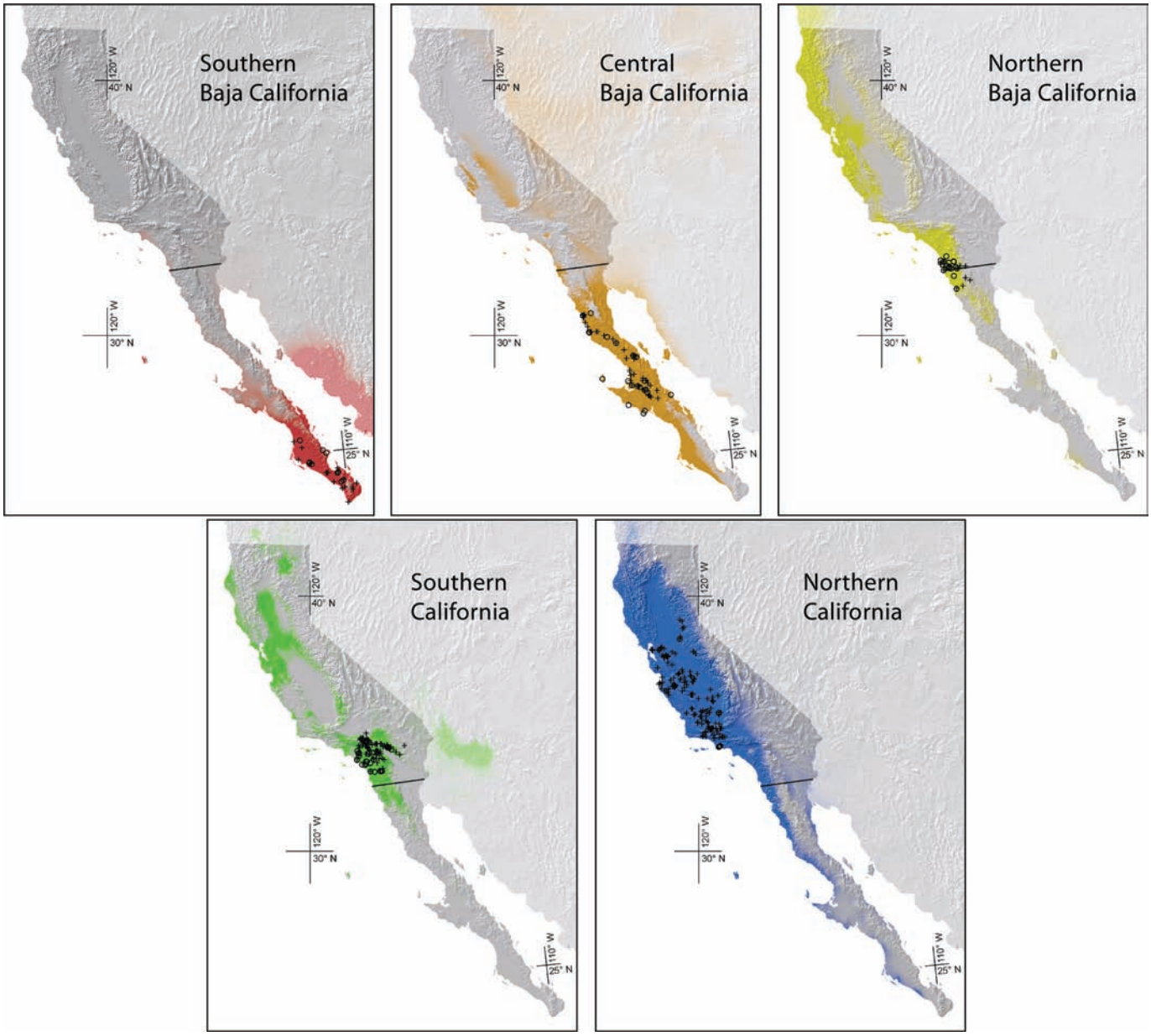

Fig. S3. Predicted distributions for the 5 phylogeographic groups within the *P. coronatum* complex. Specimens included in the genetic study are indicated by a ''○'', whereas specimens from HerpNET are indicated by a ''+.''

Table S1. Likelihood ratio tests of nested demographic models for parapatric phylogeographic groups in the *P. coronatum* complex

Model	Log likelihood	2 LLR	df	*P*
Southern California vs. Northern California				
$\theta_1\theta_2\theta_A\ m_1\ m_2$	−1.872	—	—	
$\theta_1\theta_2\theta_A\ m_1 = m_2$	−1.979	0.213	1	0.644
$\theta_1\theta_2\theta_A\ m_1 = 0\ m_2$	−1.872	0.000	1	0.492
$\theta_1\theta_2\theta_A\ m_1\ m_2 = 0$	−1.979	0.213	1	0.322
$\theta_1\theta_2\theta_A\ m_1 = m_2 = 0$	−1.978	0.212	2	0.948
Northern Baja California vs. Southern California				
$\theta_1\theta_2\theta_A\ m_1\ m_2$	−6.780	—	—	
$\theta_1\theta_2\theta_A\ m_1 = m_2$	−7.903	2.246	1	0.134
$\theta_1\theta_2\theta_A\ m_1 = 0\ m_2$	−7.904	2.247	1	0.067
$\theta_1\theta_2\theta_A\ m_1\ m_2 = 0$	−8.314	3.067	1	0.040
$\theta_1\theta_2\theta_A\ m_1 = m_2 = 0$	−11.885	10.210	2	0.078
Central Baja California vs. Northern Baja California				
$\theta_1\theta_2\theta_A\ m_1\ m_2$	−2.853	—	—	
$\theta_1\theta_2\theta_A\ m_1 = m_2$	−3.017	0.327	1	0.567
$\theta_1\theta_2\theta_A\ m_1 = 0\ m_2$	−2.951	0.196	1	0.329
$\theta_1\theta_2\theta_A\ m_1\ m_2 = 0$	−2.979	0.252	1	0.308
$\theta_1\theta_2\theta_A\ m_1 = m_2 = 0$	−2.996	0.285	2	0.912
Southern Baja California vs. Central Baja California				
$\theta_1\theta_2\theta_A\ m_1\ m_2$	−0.315	—	—	
$\theta_1\theta_2\theta_A\ m_1 = m_2$	−0.671	0.713	1	0.399
$\theta_1\theta_2\theta_A\ m_1 = 0\ m_2$	−0.670	0.711	1	0.200
$\theta_1\theta_2\theta_A\ m_1\ m_2 = 0$	−0.314	0.001	1	0.485
$\theta_1\theta_2\theta_A\ m_1 = m_2 = 0$	−0.669	0.709	2	0.836

Log-likelihood values are averages of the highest posterior probability values found across 10 replicate IMa analyses using different starting seeds. All nested models are compared with the most general model (i.e., $\theta_1\ \theta_2\ \theta_A\ m_1\ m_2$).

Table S2. Bioclimatic variables used in this study (Worldclim1.4; Hijmans et al., 2005)

ID	Variable
bio_2	Mean diurnal range [mean of monthly (max temp − min temp)]
bio_3	Isothermality
bio_7	Temperature annual range
bio_9	Mean temperature of driest quarter
bio_10	Mean temperature of warmest quarter
bio_11	Mean temperature of coldest quarter
bio_13	Precipitation of wettest month
bio_14	Precipitation of driest month
bio_15	Precipitation seasonality (coefficient of variation)
bio_18	Precipitation of warmest quarter
bio_19	Precipitation of coldest quarter

Table S3. PCA loading scores and eigenvalues for the 11 bioclimatic variables

Parameter	PC1	PC2	PC3	PC4
Eigenvalue	4.805	2.989	1.344	1.308
Percent	40.040	24.905	11.203	10.896
Cumulative percent	40.040	64.945	76.148	87.044
Latitude	−0.349	0.241	−0.287	−0.137
Mean temperature of coldest quarter	0.404	−0.213	−0.076	−0.024
Mean temperature of warmest quarter	0.387	0.203	−0.071	0.253
Isothermality	0.296	−0.266	0.204	−0.204
Mean temperature of driest quarter	0.181	0.358	−0.440	0.298
Mean diurnal range [mean of monthly (max temp − min temp)]	0.150	0.407	0.329	0.115
Precipitation of warmest quarter	0.134	−0.238	0.348	0.606
Precipitation seasonality (coefficient of variation)	−0.025	−0.327	−0.456	0.461
Temperature annual range	−0.061	0.534	0.137	0.241
Precipitation of driest month	−0.285	0.007	0.464	0.176
Precipitation of wettest month	−0.376	−0.192	−0.006	0.315
Precipitation of coldest quarter	−0.421	−0.073	−0.019	0.079

Table S4. Bioclimatic variables ranked according to their overall model contribution for the *P. coronatum* complex, separated by phylogeographic group

	Phylogeographic group									
Rank	Southern Baja California		Central Baja California		Northern Baja California		Southern California		Northern California	
1	bio_11	88.1	bio_13	44.5	bio_14	24.3	bio_14	57.6	bio_18	42.7
2	bio_15	8.1	bio_3	32.3	bio_7	23.6	bio_19	16.7	bio_19	33.1
3	bio_7	2.4	bio_7	13	bio_3	22.4	bio_3	7.9	bio_15	21.5
4	bio_2	1.1	bio_10	4.2	bio_19	20.2	bio_10	4.6	bio_13	2.7
5	bio_19	0.2	bio_2	2.2	bio_18	7.4	bio_2	3.9	bio_2	0
6	bio_9	0	bio_19	2	bio_2	1.1	bio_18	3.3	bio_9	0
7	bio_3	0	bio_18	1.6	bio_10	0.6	bio_7	2.6	bio_7	0
8	bio_18	0	bio_15	0.1	bio_15	0.3	bio_9	2.2	bio_3	0
9	bio_14	0	bio_14	0	bio_9	0.1	bio_15	1.3	bio_14	0
10	bio_13	0	bio_9	0	bio_13	0	bio_13	0	bio_11	0
11	bio_10	0	bio_11	0	bio_11	0	bio_11	0	bio_10	0
Highest gain	bio_11		bio_3		bio_3		bio_14		bio_18	
Lowest gain	bio_11		bio_7		bio_14		bio_14		bio_18	
AUC	0.96 ± 0.008		0.917 ± 0.009		0.888 ± 0.04		0.942 ± 0.008		0.816 ± 0.011	

The "area under the curve" (AUC) statistic suggests that the models predicted for the phylogeographic groups are robust. The variables with the highest gain are the most important in model generation, whereas those with the lowest gain indicate that, when withheld from the model, that particular variable could not be compensated for by the other variables. Bioclim variables are as follows: bio_2, mean diurnal range [mean of monthly (max temp − min temp)]; bio_3, isothermality; bio_7, temperature annual range; bio_9, mean temperature of driest quarter; bio_10, mean temperature of warmest quarter; bio_11, mean temperature of coldest quarter; bio_13, precipitation of wettest month; bio_14, precipitation of driest month; bio_15, precipitation; seasonality (coefficient of variation); bio_18, precipitation of warmest quarter; bio_19, precipitation of coldest quarter.

Table S5. Locality data and voucher numbers for *P. coronatum* complex specimens included in the study

Locality code	Locality	Latitude	Longitude	Nucleotide sequence data					Voucher no.
				12S	*ND1ND2*	*RAG–1*		*BDNF*	
	Mexico: Baja California Norte								
BCN-1	10.9 mi N Correo	30.06666	−115.75000	X	X	X	—	—	RWM 543
BCN-2	12.9 mi S Catavina	29.58333	−114.56667	X	X	X	X	X	MVZ 161208
BCN-3	18 mi S Catavina	29.84053	−114.95000	X	X	X	X	X	RWM 1243
BCN-4	2 mi S El Arco	28.01667	−113.41667	X	X	X	X	X	BYU 34878
BCN-5	2.8 km E El Rosario, Bridge crossing Rio Del Rosario	30.05000	−115.73333	X	X	X	X	X	ROM 13536
BCN-6	21.1 mi W Bahia de Los Angeles	29.05167	−113.85167	X	X	X	X	X	MVZ 161206
BCN-7	47 km E Hwy 1 on road to Bahia de Los Angeles	28.98511	−113.71215	X	X	X	X	X	MVZ 161207
BCN-8	Cedros Island	28.20000	−115.25000	X	X	X	X	X	WLHMX 1017
BCN-9	Colonia Guerrero	30.73472	−115.99111	X	X	X	X	X	MVZ 161187
BCN-10	Colonia Guerrero	30.73472	−115.99111	X	X	X	X	X	MVZ 161188
BCN-11	Ensenada, El Cerro	31.80243	−116.55892	X	X	X	X	X	UABC 1334
BCN-12	Guerrero Negro	28.05000	−114.13333	X	X	X	—	—	RWM 1817
BCN-13	Sierra San Pedro Martir, Rancho San Antonio Murillos	30.81168	−115.63200	X	X	X	—	—	UABC 1216
BCN-14	Valle las Palmas, Microondas Cerro Bola	32.31342	−116.65738	X	X	X	X	X	UABC 1304
	Mexico: Baja California Sur								
BCS-1	1 km N Santa Rita	24.60155	−111.47480	X	X	X	X	X	UABC 1007
BCS-2	1.3 mi NE Punta Abreojos	26.73649	−113.55919	X	X	X	X	X	CAS 147740
BCS-3	1.8 mi S El Triunfo	23.78333	−110.13333	X	X	X	X	X	ROM 13292
BCS-4	11 km S Santa Rita	24.54338	−111.37488	X	X	X	X	X	SD Field 251
BCS-5	132 km N Santa Rosalia	27.55783	−113.33810	X	X	X	X	X	UABC 997
BCS-6	2.1 mi S junction of road to El Arco and Hwy 1	27.83667	−113.72833	X	X	X	X	X	MVZ 161212
BCS-7	2.5 mi NW San Evaristo Base Camp	24.93152	−110.73282	X	X	X	X	X	SD Field 530
BCS-8	25.9 mi E Guerrero Negro	27.78333	−113.64166	X	—	X	—	—	CAS 147787
BCS-9	30 mi. S La Paz	23.73047	−110.22639	X	X	X	X	X	RPM 2479
BCS-10	38.9 mi W San Ignacio	27.66660	−113.38333	X	—	X	—	—	RWM 1242
BCS-11	5 km E La Paz	24.09548	−110.34352	X	X	X	X	X	UABC 1053
BCS-12	7.5 mi S Guerrero Negro	27.88250	−113.97972	X	X	X	X	X	MVZ 161210
BCS-13	9 km N Santa Rosalia	27.39153	−112.32210	X	X	X	X	X	UABC 1075
BCS-14	9 mi N Punta Abreojos	26.83254	−113.49401	X	X	X	X	—	RWM 1068
BCS-15	La Paz, El Sombrero Trailer Park	24.14222	−110.31083	X	X	X	X	X	MVZ 137778
BCS-16	Los Dolores	25.06273	−110.86720	X	X	X	X	X	UABC 1092
BCS-17	Piedras Paradas	25.52504	−111.79269	X	X	X	X	X	SDSNH 620
BCS-18	Santa Rita	24.61670	−111.46670	X	X	X	X	X	SDSNH
BCS-19	Vizcaino	27.64778	−113.44250	X	X	X	X	X	MVZ 161213
BCS-20	Vizcaino	27.64778	−113.44250	X	X	X	X	X	MVZ 161214
BCS-21	Vizcaino Desert, Asuncion Flats	27.10000	−114.18330	X	X	X	—	—	SDSNH
	USA: California								
AMD-1	Amador County, Lone-Buena Vista Rd., 0.5mi N Hwy. 88	38.32696	−120.92941	—	—	X	—	—	MVZ 179812
KRN-1	Kern County, Lerdo Hwy., 3.5 mi W I-5	35.49938	−119.59663	X	X	X	X	X	MVZ 150066
KRN-2	Kern County, Magnolia and 7th Streets jct. on Standard Rd.	35.44088	−119.02091	X	X	X	X	X	MVZ 161471
KRN-3	Kern County, Magnolia and 7th Streets jct. on Standard Rd.	35.44088	−119.02091	X	X	X	X	X	MVZ 161472
LA-1	Los Angeles County, Mescal Creek, N of Angeles N.F.	34.42600	−117.71010	X	X	X	X	X	PHCO-RY 2
LA-2	Los Angeles County, Piru Creek	34.57465	−118.77593	X	X	X	—	—	ROM 23292
MTRY-1	Monterey County, China Camp	36.29589	−121.56714	X	X	X	X	X	MVZ 230680
ORNG-1	Orange County, Loma Ridge	33.73769	−117.69377	X	X	X	X	X	MVZ 249247
ORNG-2	Orange County, NE Weir Canyon	33.83824	−117.72276	X	X	X	—	—	PHCO-WEI 500
ORNG-3	Orange County, NE Weir Canyon	33.83824	−117.72276	X	X	X	X	X	PHCO-WEI 502
ORNG-4	Orange County, NW Gilman Peak	33.92821	−117.76606	X	X	X	X	X	PHCO-CHI 24
ORNG-5	Orange County, San Joaquin Hills	33.59710	−117.79636	X	X	X	X	X	MVZ 249256
ORNG-6	Orange County., Santa Ana Mountains, ridge SW Coal Canyon	33.85462	−117.68777	X	X	X	X	X	PHCO-CHI 15
ORNG-7	Orange County, West San Joaquin Hills	33.57901	−117.79314	X	X	X	—	—	PHCO-SJHW 3
RVRS-1	Riverside County, Diamond Valley, base of ″North Hills″	33.69394	−116.98611	X	X	X	X	X	CAS 200652
RVRS-2	Riverside County, Diamond Valley, base of ″North Hills″	33.69394	−116.98611	X	X	X	X	X	CAS 200653
RVRS-3	Riverside County, Joshua Tree, S Lost Horse Valley	33.94760	−116.17166	—	X	X	—	—	PHCO-JOS 5000
RVRS-4	Riverside County, Joshua Tree, Upper Covington Flat	34.03091	−116.34881	X	—	X	X	X	PHCO-COV 04
RVRS-5	Riverside County, Joshua Tree, Upper Covington Flat	34.02600	−116.33915	X	X	X	X	X	PHCO-COV 13
RVRS-6	Riverside County, Lake Perris State Recreation Area	33.86638	−117.19469	X	X	—	X	X	PHCO-PERRIS

Locality code	Locality	Latitude	Longitude	Nucleotide sequence data					Voucher no.
				12S	*ND1*	*ND2*	*RAG–1*	*BDNF*	
RVRS-7	Riverside County, Lake Skinner	33.58192	−117.01892	—	X	X	—	—	MVZ 249251
RVRS-8	Riverside County, Perris Valley	33.80880	−117.25502	X	X	X	X	X	PHCO-MOT 132
RVRS-9	Riverside County, Santa Margarita Ecological Reserve	33.43883	−117.17980	X	X	X	—	—	PHCO-SMER11
RVRS-10	Riverside County, Santa Margarita Ecological Reserve	33.44635	−117.17191	X	X	X	X	X	PHCO-SMER4
RVRS-11	Riverside County, SE Tenaja Canyon	33.51040	−117.36875	X	X	X	X	X	PHCO-TEN 31
RVRS-12	Riverside County, Tenaja Corridor	33.50311	−117.33704	X	—	—	—	—	PHCO-TEN 3
SBNT-1	San Benito County, Pinnacles N.M.	36.49238	−121.14838	X	X	X	X	X	RNF 2849
SNBRN-1	San Bernardino County, Joshua Tree, Lower Covington Flat	34.05661	−116.32574	X	—	X	—	—	PHCO-COV 23
SNBRN-2	San Bernardino County, N San Bernardino foothills	34.33703	−117.31689	X	X	X	X	X	MVZ 249246
SNBRN-3	San Bernardino County, Silverwood Lake S.R.A.	34.28039	−117.35906	X	X	X	X	X	PHCO-SILVER02A
SNBRN-4	San Bernardino County, Silverwood Lake S.R.A.	34.30301	−117.33465	X	X	X	—	—	PHCO-SILVER02B
SNBRN-5	San Bernardino County, Silverwood Lake S.R.A.	34.30301	−117.33465	X	X	X	X	X	PHCO-SILVER21
SD-1	San Diego County, Border Field State Park	32.54573	−117.12354	X	X	X	X	—	MVZ 249257
SD-2	San Diego County, Border Field State Park	32.54573	−117.12354	X	X	X	—	—	MVZ 249258
SD-3	San Diego County, Boulder Creek	32.86170	−116.64130	X	X	X	X	X	SDSNH 68905
SD-4	San Diego County, Camp Pendleton	33.37420	−117.43678	—	—	X	—	—	PHCO-PEN
SD-5	San Diego County, Camp Pendleton	33.38988	−117.56260	X	—	X	X	X	PHCO-PEN1
SD-6	San Diego County, Camp Pendleton	33.41584	−117.37224	X	X	X	X	X	PHCO-PEN15
SD-7	San Diego County, Campo	32.59690	−116.50591	—	X	X	—	—	MVZ 249260
SD-8	San Diego County, Cleveland N.F., Upper Poverty Gulch,	32.88349	−116.65015	—	X	—	—	—	PHCO-EE 02–131872
SD-9	San Diego County, La Cresta	32.84088	−116.87195	X	—	—	—	—	PHCO-CRESTA
SD-10	San Diego County, Little Cedar Ridge	32.62632	−116.86501	X	X	X	—	—	PHCO-LC05
SD-11	San Diego County, Little Cedar Ridge	32.62524	−116.86346	X	X	X	—	—	PHCO-LC15
SD-12	San Diego County, Marron Valley Rd.	32.59511	−116.76700	X	X	X	X	X	MVZ 249248
SD-13	San Diego County, Miramar Naval Air Station	32.89063	−117.10260	X	—	X	—	—	PHCO-Elliot 503
SD-14	San Diego County, Rancho Jamul	32.67965	−116.86771	X	X	X	—	—	PHCO-RJ04
SD-15	San Diego County, Rancho Jamul	32.67306	−116.85371	X	X	X	—	—	PHCO-RJ11
SD-16	San Diego County, S Hauser Canyon	32.65872	−116.55120	X	X	X	X	X	SD Field 335
SD-17	San Diego County, San Diego National Wildlife Refuge	32.72050	−116.95012	X	X	X	X	X	PHCO-SDNWR0202
SD-18	San Diego County, San Marcos	33.11390	−117.18190	X	X	X	X	X	MVZ 249259
SD-19	San Diego County, Santa Ysabel Ecological Reserve	33.11260	−116.64715	X	X	X	—	—	PHCO-SYR100
SD-20	San Diego County, Santa Ysabel Ecological Reserve	33.10291	−116.70272	X	X	X	X	X	PHCO-SYR23
SD-21	San Diego County, Santa Ysabel Ecological Reserve	33.13186	−116.71966	—	X	X	—	—	MVZ 249249
SD-22	San Diego County, Torrey Pines	32.94082	−117.24776	X	X	X	X	X	PHCO-TP 14
SD-23	San Diego County, Torrey Pines	32.94142	−117.25045	X	X	X	—	—	PHCO-TP 141
SD-24	San Diego County, University of California Elliot Reserve	32.89167	−117.10833	X	X	X	X	X	MVZ 249254
SD-25	San Diego County, University of California Elliot Reserve	32.89167	−117.10833	X	X	—	—	—	MVZ 249255
SD-26	San Diego County, Wild Animal Park	33.09471	−116.98417	X	X	X	X	X	PHCO-WAP 21
SD-27	San Diego County, Wild Animal Park	33.09613	−116.98005	X	X	X	X	X	PHCO-WAP 232
VNTR-1	Ventura County, E La Jolla Valley	34.10150	−119.03548	X	X	X	X	X	PHCO-LJV 28
VNTR-2	Ventura County, NE Big Sycamore Canyon	34.14642	−118.96578	X	X	X	X	X	PHCO-SYC 33
VNTR-3	Ventura County, Ridge btwn. Wood and Big Sycamore Canyons	34.13589	−119.00037	X	X	X	X	X	PHCO-SYC 37
VNTR-4	Ventura County, SE La Jolla Peak	34.11008	−119.028	X	X	X	X	X	PHCO-LJV 23

Locality codes correspond to the taxon labels used in the phylogenetic analyses (Fig. S1). Molecular data collected for individuals are indicated with an "X," and missing data are denoted with an "—". Standard museum abbreviations follow Leviton et al. (1985). Nonstandard abbreviations and field series abbreviations are as follows: UABC, Universidad Autónoma de Baja California; SD Field, San Diego Natural History Museum Field Series; PHCO, USGS San Diego Field Station; RNF, Robert N. Fisher; RPM, Richard P. Montanucci; RWM, Robert W. Murphy; WLHMX, Wendy L. Hodges.

Table S6. Molecular data partitions, character variation, and the nucleotide substitution model selected for each partition using the Akaike Information Criterion

Data partition	Characters	Variable characters	Parsimony informative characters	Percent parsimony informative	Substitution model
12S rRNA	752	71	48	6.38	GTR+I+Γ
ND1–first codons	323	36	29	8.98	GTR+I+Γ
ND1–second codons	323	12	5	1.54	HKY+I
ND1–third codons	323	144	122	37.78	GTR+I+Γ
ND2–first codons	345	68	46	13.33	GTR+Γ
ND2–second codons	344	27	16	4.65	HKY+I+Γ
ND2–third codons	344	154	123	35.76	GTR+I+Γ
RAG–1	1054	15	6	0.57	GTR
BDNF	529	6	4	0.76	GTR+I

Outgroup taxa were excluded prior to all calculations.

Table S7. Voucher specimen numbers for *P. coronatum* samples included in the geometric morphometric analyses

Females	Males
CAS: 5650, 5651, 7208, 11619, 11620, 12041, 12936, 12938, 17651, 17655, 17656, 22769, 22770, 22771, 27723, 27782, 39081, 40127, 40132, 40149, 40156, 40209, 40212, 40215, 40217, 40219, 40220, 43075, 43076, 43077, 43276, 43410, 43577, 44000, 44106, 46833, 46834, 48894, 58057, 58127, 58128, 58131, 58150, 58153, 64652, 64653, 71327, 71969, 71971, 71972, 74619, 74620, 84230, 84786, 84790, 84804, 85101, 92165, 143851, 143852, 143854, 143855, 143861, 143865, 145185, 145187, 145189, 145191, 145192, 145193, 145194, 147787, 152096, 152099, 152227, 152230, 181378, 181382, 181386, 181394, 181395, 181397, 181403, 181404, 181405, 181406, 181409, 181416, 189973, 189974, 189975, 189976, 189979, 195010, 197514, 201787. CAS-SU: 39, 40, 43, 46, 49, 72, 78, 83, 179, 180, 1112, 1991, 3321, 3331, 3697, 5524, 5525, 5526, 5652, 5748, 5749, 5751, 5752, 7208, 7922, 7923, 7924, 10033, 11374, 12929, 12931, 12934, 12944, 12948, 12949, 18824. MVZ: 11735, 11740, 11748, 11749, 11750, 11751, 11752, 11761, 11763, 13634, 13635, 37319, 37320, 37324, 37326, 37328, 37330, 45389, 50071, 50073, 50074, 51095, 51097, 51132, 73555, 75890, 100473, 117321, 117323, 117324, 140821, 140822, 140824, 140825, 150070, 161192, 161194, 161199, 161200, 161202, 161206, 161209, 161211, 161212, 161213, 161214, 161218, 161220, 161222, 161223, 161226, 161228, 161229, 161237, 161239, 161241. USNM: 154, 7908, 10779, 12664, 18447, 18448, 18451, 18456, 18458, 18459, 21965, 21973, 21984, 21990, 21993, 23695, 34614, 37583, 44601, 44602, 44603, 44861, 44878, 44879, 44947, 45136, 46809, 53689, 53692, 53694, 53695, 53696, 53698, 53700, 56865, 56871, 59839, 64285, 64286, 64450, 64465, 131658, 196520, 240257, 240262, 240264, 240332, 240592, 293194, 293199, 293201, 293220, 293221, 293223, 293224, 293239, 293245.	CAS: 1651, 1659, 3325, 12928, 12937, 12939, 12940, 12945, 12946, 17649, 17652, 17653, 17654, 17657, 20935, 22084, 22085, 23039, 27305, 27522, 35360, 38995, 38996, 39862, 40001, 40126, 40128, 40129, 40133, 40134, 40137, 40138, 40144, 40151, 40154, 40193, 40203, 40205, 40210, 40213, 40218, 41701, 42041, 43099, 43324, 43325, 43428, 43561, 46832, 46839, 48895, 50475, 57609, 58032, 58130, 58151, 63967, 64651, 64968, 71970, 84697, 84784, 84946, 90198, 90530, 143423, 143432, 143848, 143849, 143857, 143858, 145173, 145174, 145175, 145188, 145190, 145195, 145196, 147474, 147475, 147684, 147755, 152097, 152098, 152228, 152229, 152231, 181374, 181383, 181389, 181392, 181398, 181402, 181407, 181408, 181410, 181412, 181413, 181414, 181415, 189967, 189968, 189970, 189971, 189972, 189977, 189986, 189988, 189989, 189992, 195008, 197513, 201788, 223658. CAS-SU: 47, 68, 71, 80, 82, 177, 178, 3115, 3439, 5523, 5851, 6163, 6377, 6511, 11377, 11926, 12927, 12930, 12932, 12941, 12942. MVZ: 9776, 9777, 10660, 11736, 11737, 11743, 11745, 11747, 11755, 11758, 11766, 13625, 13626, 13629, 13636, 13638, 37334, 50075, 50076, 73551, 73554, 73556, 73557, 117316, 117317, 117318, 117319, 117320, 117463, 117464, 117465, 140823, 140826, 150068, 150069, 150073, 150074, 161188, 161189, 161190, 161195, 161196, 161197, 161198, 161201, 161203, 161204, 161216, 161217, 161219, 161221, 161230, 161233, 161234, 161238, 161240, 182262. USNM: 156, 157, 4587, 10780, 12618, 13948, 14587, 18452, 18457, 21966, 21967, 21985, 21988, 21991, 32335, 34613, 34617, 34618, 37584, 37585, 44807, 44853, 45137, 46808, 46888, 53599, 53688, 53690, 53698, 53701, 53702, 54842, 55105, 56866, 59841, 75137, 75138, 131657, 146460, 240255, 240258, 240259, 240263, 240329, 240330, 240331, 240333, 240334, 240335, 240337, 293196, 293200, 293202, 293206, 293208, 293216.

Museum abbreviations are as follows: CAS/ CAS-SU, California Academy of Sciences; MVZ, Museum of Vertebrate Zoology; USNM, National Museum of Natural History.